

Corrosion Resistance of Stainless Steels in Chloride Containing Supercritical Water Oxidation System

Young Sik Kim[†], D. Bryce Mitton* and Ronald M. Latanision*

Department of Materials Science and Engineering, Andong National University,
388 Songchun, Andong 760-749, Korea

*The H. H. Uhlig Corrosion Laboratory, MIT, 77 Massachusetts Avenue, Cambridge, MA, 02139, USA

(Received 26 August 1999 • accepted 28 October 1999)

Abstract—As the science and process applications of supercritical water (SCW) and supercritical water oxidation (SCWO) become more thoroughly understood, it is logical to envision the use of the SCWO process by diverse industries and public wastewater and sludge generators. This technology can be adapted to accomplish either pre or end-of-pipe wastewater treatment. There is a need to destroy both military and civilian hazardous waste, and urgency, mandated by public concern over traditional waste handling methodologies, to identify safe and efficient alternative technologies. By capitalizing on the properties of water above its critical point, 374 °C and 22.4 MPa for pure water, this technology provides rapid and complete oxidation with high destruction efficiencies at typical operating temperatures. Nevertheless, corrosion of the materials of fabrication is a serious concern. While iron-based alloys and nickel-based alloys are generally considered important for service applications, results from laboratory and pilot-scale SCWO systems presently in operation indicate that they will not withstand some aggressive feeds. Significant weight loss and localized effects, including stress corrosion cracking (SCC) and dealloying, are seen in chlorinated environments. This work assesses the corrosion characteristics of iron-based stainless steels exposed to high supercritical temperatures in a chlorinated military waste containing salts.

Key words: Supercritical Water Oxidation, Military Waste, High Temperature Corrosion, Austenitic Stainless Steel, Duplex Stainless Steel, EIS, Anodic Polarization Test

INTRODUCTION

The major disadvantages of SCWO revolve around high pressure ($P > 230 \times 10^5 \text{ N/m}^2$), potential solids handling problem, and, for some waste streams, corrosion [Tester et al., 1993]. Although SCWO is technologically able to destroy hazardous wastes, the process must be carried out in a reactor capable of accommodating elevated temperatures, pressures and, potentially, a very aggressive environment.

In general, AISI type 316 L stainless steel has been employed as a baseline material during SCWO testing. In deionized water, it may exhibit (i) general corrosion and excellent overall performance [Tebbal and Kane, 1998], (ii) pitting (400 °C and 24.5 MPa) [Boukis et al., 1995], (iii) intergranular (300 °C, 3,600 psi) [Mitton et al., 1995] or (iv) crevice corrosion (at the periphery of a mounting washer 500 °C, 3,600 psi) [Mitton et al., 1996]. In more aggressive feed stream, 316L may exhibit (i) relatively good performance (500 °C over the pH range 2-11 and minimal Cl⁻) [Tebbal and Kane, 1998], (ii) general corrosion (0.05 mol/l HCl, no added oxygen) [Boukis et al., 1995], (iii) wastage (~2000 mpy) and cracking (600 °C in a highly chlorinated organic feed stream) [Mitton et al., 1996], (iv) pitting and crevice corrosion [Thomas and Gloyna, 1991] or SCC under alkaline conditions (pH > 12) [Tebbal and Kane, 1998].

High nickel materials are frequently recommended for severe

service application [ASM, 1987] and have, therefore, been utilized during fabrication for a number of bench-scale and pilot plant reactors. Notwithstanding this, the current data base suggests that these materials are not likely to be capable of handling conditions associated with aggressive SCWO feed streams [Latanision and Shaw, 1993; Tebbal and Kane, 1998; Mitton et al., 1995a, b, 1996b; Orzalli, 1994; Norby, 1993; Latanision, 1995; Kane and Cuellar, 1994]. In deionized water, Inconel-625 primarily exhibits oxide layer development both at 400 °C [Boukis et al., 1995] and 500 °C [Mitton et al., 1995a]. Some minor pitting has also been reported at 500 °C [Mitton et al., 1995a]. In more aggressive feed streams various investigators have reported (i) general corrosion at 0.05 mol/l (1,800 ppm) HCl no added oxygen [Boukis et al., 1995], and (ii) dealloying of both I-625 [Rice et al., 1993; Bramlette et al., 1990] and C-276 [Latanision, 1995; Mitton et al., 1996b; Bramlette et al., 1990]. More worrying, however, are the numerous reports of SCC: (i) cracking of I-625 (300 °C) but not of C-276 exposed to 0.5 mol/l, 18,000 ppm HCl [Boukis et al., 1995] and cracking of C-276 exposed to aqueous methylene chloride [Latanision, 1995]. Both transgranular and intergranular cracking is observed at subcritical, but not at supercritical, temperatures when exposed to complex low pH conditions [Zilberstein et al., 1995]. In addition, cracking is reported when I-625 is exposed to a mixed methylene chloride isopropyl alcohol feed neutralized with NaOH after extended times at supercritical temperatures (300 hours at 580 °C) [Latanision and Shaw, 1993]. At high supercritical temperatures, in the absence of salt precipitation there is an indication that corro-

[†]To whom correspondence should be addressed.

E-mail: yikim@andong.ac.kr

Table 1. The composition and nomenclature for a number of chemical agents

Agent acronym/ Name	Composition
GB (Sarin)	Isopropyl methylphosphonofluoridate
VX	O-ethyl S-diisopropylamino-methyl methylphosphonothiolate
HM (Mustard)	Bis-2-(Chloroethyl) sulfide
GF	Cyclohexyl methylphosphonofluoridate
GD (Soman)	Pinacolylmethyl-phosphonofluoridate
GA (Tabun)	O-ethyl dimethyl-amidophosphoryl cyanide

sion may be minimal both for unstressed C-276 [Mitton et al., 1998] and stressed C-276 and I-625 [Tebbal and Kane, 1998] samples. The current paper assesses primarily samples exposed to supercritical temperatures in a highly chlorinated salt producing environment.

There is in excess of 23,000 tons of chemical agent stockpiled (characterized and stored in a controlled environment) at eight sites within the continental USA. The composition and nomenclature for a number of agents are presented in Table 1 [The NATO, 1994]. While production was stopped in the late 60's, some of this waste may have originated as long ago as the last world war [Drake, 1993]. In addition to stockpiled munitions, there exists a significant, but unknown, quantity of non-stockpiled waste that also needs to be considered for destruction [Aqua forties, 1993]. This non-stockpiled waste (all chemical agent materials outside the stockpiled [Aqua forties, 1994]) is a growing technical challenge because of the variety and circumstances in which it is found [The NATO, 1994]. These chemicals are found occasionally during excavations or washed up on the beach etc. [Aqua forties, 1994]. For example, shells containing chemical agents were uncovered in a residential suburb in Washington, D.C. of the USA; and both the "O" field in Edgewood MD and the Dugway proving ground are known to have significant quantities of agent-containing munitions [Aqua forties, 1993]. The Chemical Weapons Convention (CWC) [The Convention, 1994], which was signed by 130 countries (January 1993) seeks to eliminate chemical weapons and their production early in the new millennium [Drake, 1993; Aqua forties, 1993b]. In order to be able to accomplish this, a safe, efficient and economical waste disposal methodology needs to be identified. While a number of traditional destruction methodologies such as landfill or incineration do currently exist, they face significant public opposition. For instance, although incineration is widely employed to destroy waste, it has resulted in serious public concern as a consequence of stack emissions and other problems. Further, the economics of incineration require a relatively high concentration of waste in the waste stream and the previous practice of permitting aqueous waste concentration by evaporation in open ponds prior to disposal is no longer acceptable. The clean up of military and civilian hazardous wastes is, nevertheless, gaining national importance [Swallow and Ham, 1993].

In addition to chemical agents, there is a need for the United States Department of Energy (DOE) to address the clean-up of more than 160,000 m³ of mixed waste in its charge. While SCWO is demonstrably capable of destroying such wastes, many of the

DOE wastes contain solvents or oils that are high in chlorine or other potentially corrosive precursors (e.g., fluorine, sulfur, tributyl phosphate). During destruction by SCWO, these can be oxidized to acidic products. In the case of chemical agents, the oxidation of GB (Sarin) produces a mix of hydrofluoric and phosphoric acids; the oxidation of VX results in sulfuric and phosphoric acids; and finally, the oxidation of HD (mustard agent) produces hydrochloric and sulfuric acids [Swallow et al., 1995]. Such acidic conditions may result in significant corrosion of the process unit and, in the context of the development of scaled-up systems [Latanision and Shaw, 1993; Mitton et al., 1993, 1994], corrosion may ultimately be the deciding factor in the commercial application of this technology.

After SCWO testing, specimens were covered with thick salt layer and thin oxide layer. Because this supercritical water includes metallic constituents and its temperature was very high, corrosion processes on the surface would be complicated. Generally, oxide film can protect the matrix surface from chemical and electrochemical attack. However, it is difficult to monitor the corrosion process *in-situ* since supercritical water oxidation testing is performed at high temperature and high pressure. So, this work performed SCWO test for austenitic and duplex stainless steels. AC impedance measurement and DC polarization test were performed in high chloride acidic solution for oxide-covered samples after SCWO test and base metals. The objective of this work is to compare and elucidate the properties of the oxide layer and base metal.

EXPERIMENTAL PROCEDURE

1. Supercritical Water Oxidation Test

Fig. 1 shows the corrosion racks of supercritical water oxidation testing used in this work. SCWO testing condition can be summarized as follows: test temperature is 600 °C and test pressure is about 3,300 psig and test duration is 66.2 hours, but hot time is 90.2 hours. Test facility is No. 7 MODAR in General Atomic of USA. The conditions of test solution are very complicated and are shown in several tables.

2. Specimen

In this work, two kinds of sample, such as base and welded metal, were used. Typical chemical compositions are as follows:

M, W, and O after an alloy's name reveal the history of the materials such as base metal, welded metal, and oxide-covered samples, respectively.

Specimen thickness is 3 mm and its length is 50 mm and its width is 20 mm. The center of the specimen is drilled at radius of 10 mm and this hole is used to stack the specimen.

3. Microstructural Observation and Hardness Test

Specimen is ground by using an SiC paper and polished to 1 μm diamond paste. Grinding is performed as a wet process for oxide-covered samples. OM (Optical Microscope) and SEM (Scanning Electron Microscope) observations were done and compositional distribution was detected by using a WDS (Wavelength Dispersive Spectroscopy). Hardness is measured for non-SCWO tested and SCWO tested samples by using a Vickers Hardness tester.

4. *Ex-situ* Electrochemical Measurement

Using EIS (Electrochemical Impedance Spectroscopy), open

circuit potential and impedance data are obtained. Testing solution is 0.5 N HCl+1 N NaCl. This solution was intended to simu-

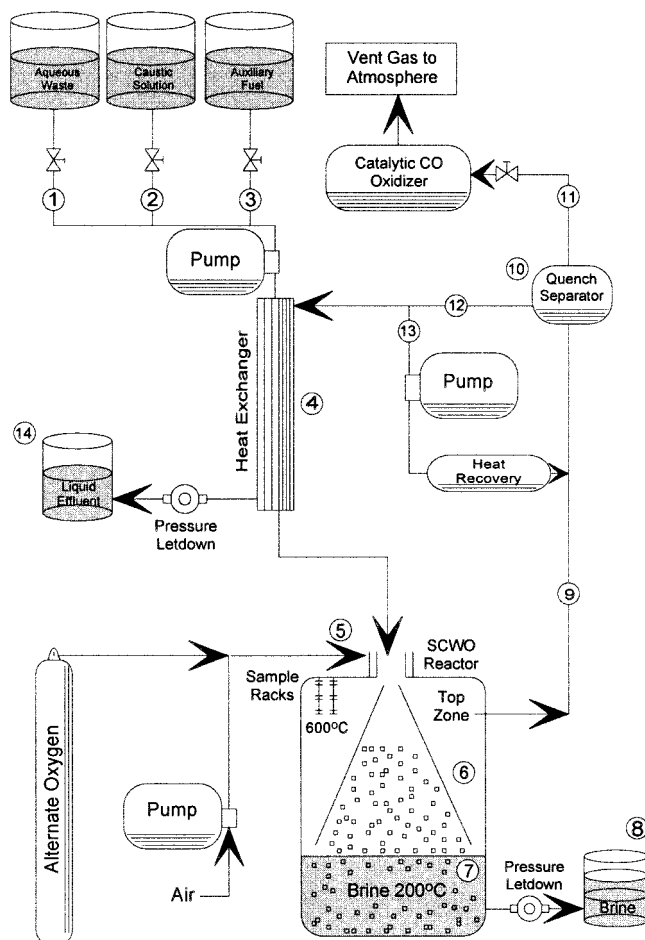


Fig. 1. A schematic diagram of a waste treatment system based on SCWO technology.

Table 2. Input flow rate of SCWO

Constituents	Air	SCW	Metals	Trimsol	Total
Rate (g/min)	839	1,160	160	62	2,221

Table 3. Metal composition (Metal acetates dissolved in water)

Elements	Ce	Zn	Pb	Ca	Fe
mg/kg	1,450	656	809	145	48

Table 4. Trimsol composition I

Elements	C	H	O	N	Cl	S
wt%	65.99	10.70	10.69	0.21	11.08	1.33

Table 8. Chemical composition of experimental alloys (wt%)

Alloys	Cr	Mo	N	C	Ni	Si	Mn	P	S	Cu	Fe	PRE*
316L	18.0	2.5	-	0.03	12.0	1.0	2.0	0.045	0.03	-	Bal.	26.3
F255	25.0	3.8	0.23	0.04	6.5	1.0	1.5	0.04	0.03	1.5	Bal.	44.4

*PRE (Pitting Resistance Equivalent)=%Cr+3.3(%Mo+0.5%W)+30%N

late high chloride solution of SCW and an HCl solution was added to increase the corrosion. Testing temperature was room temperature. AC impedance was measured at open circuit potential from 60 kHz to 5 mHz by using a Schlumberger Solatron 1,250 Frequency Response Analyzer (FRA) in combination with a Solatron 1286 potentiostat. Oxide-covered sample was made after the salt-layer was completely removed by using an ultrasonic cleaning. Samples (Base and weld metal) that were not tested in supercritical water oxidation were ground to #600 SiC paper.

A DC polarization test was performed for base metal (ground to #600 SiC paper) and oxide-covered samples and a Potentiostat (EG&G Model 273) was used. Testing solution is 0.5 N HCl+1 N NaCl. It was done at room temperature. After immersion of samples, all samples were held for 20 minutes at open circuit potential and then were polarized at a scanning rate of 1 mV/sec.

RESULTS AND DISCUSSION

1. Corrosion Behavior in the SCWO Test and the Acidic Chloride Solution

Fig. 2 shows the corrosion rate of austenitic and duplex stainless steels obtained from supercritical water oxidation test. F255 (Ferralium-255) that is Fe-base duplex stainless steel shows relatively good corrosion resistance, and the corrosion rate of typical austenitic stainless steel, 316L shows the highest value. In this work, a welded sample means that the specimen has welded area, but this does not imply the only welded area (the width of welded area: ca. 6 mm). In case of austenitic stainless steel 316L, the corrosion rate of non-welded sample was bigger than that of the welded sample. According to optical microscopic observation on corroded samples of 316L, the welded area was less corroded apparently than the non-welded sample. Even though the scattering of corrosion rate is considered, it should be noted that the welded area could affect corrosion in SCWO because its area has dendritic structure in austenitic stainless steel 316L.

Table 5. Trimsol composition II

Elements	Na	K	Si	F
mg/kg	5,525	1,986	46	29

Table 6. Reactor composition I

Species	N ₂	O ₂	CO ₂	H ₂ O	Total
wt%	29	6	7	58	100

Table 7. Reactor composition II

Species	Cl	S	Na	K	Si	F	Ce	Zn	Pb	Ca	Fe
mg/kg	3,093	371	154	55	1	1	104	47	58	10	3

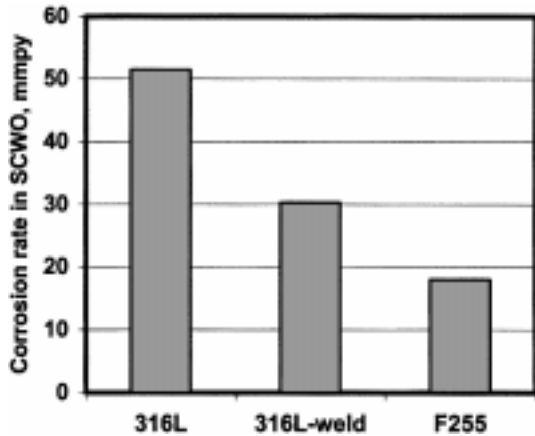
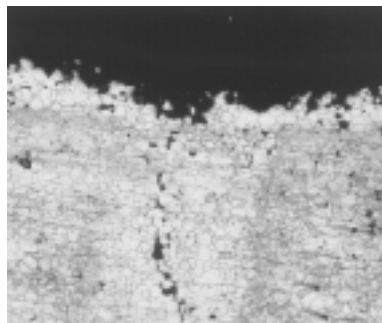
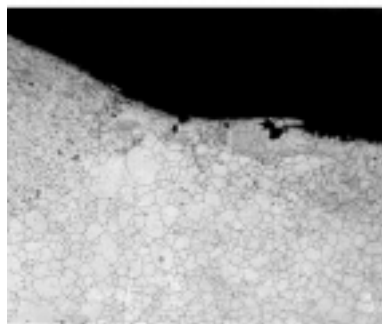


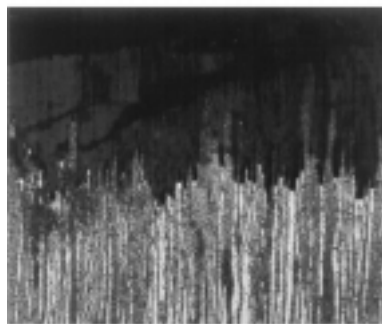
Fig. 2. Corrosion rate of duplex and austenitic stainless steels in SCWO test.



(a) 316L-base metal



(b) 316-welded area



(c) F255

Fig. 3. Corrosion morphologies (magnification $\times 100$) of austenitic stainless steel 316L and duplex stainless steel F255 after SCWO test.

Fig. 3 shows the optical microstructures on corrosion morphologies of austenitic stainless steel 316L and duplex stainless steel

F255. In base metal of 316L, some cracks were observed and its cracking mode was intergranular type. The surface was severely corroded and the surface area was degraded by intergranular corrosion. On the other hand, the welded area of 316L was less corroded, and this result can support the difference of corrosion rate between the base metal and welded samples as shown in Fig. 2. Duplex stainless steel F255 shows different morphologies to the former 316L alloy. A stable layer was formed along the rolling direction. It is believed that the formation of the surface layer was closely related to the phase of matrix.

We can summarize the results of corrosion rate and morphologies: (1) A stable layer was formed on the surface of high resistant alloys in the SCWO test; (2) The alloys showing stable layer on the surface reveal good corrosion resistance in the SCWO test.

What is the key factor to control the corrosion rate in the SCWO test? First, because testing temperature is high and testing solution is fed at 2.2 kg/min in this SCWO testing condition, the materials would be transformed to the microstructure with hard phases, and also the hardness of the samples can affect the corrosion rate in SCWO test. Fig. 4 shows the relationship between corrosion rate in SCWO test and hardness of sample before/after SCWO test of Fe-base alloys. Not like Ni-base alloys [Kim, 1999], there is a relatively linear relationship between them, but it is difficult to explain that the hardness did affect directly the corrosion behavior in the SCWO system, because the phase and the corrosion morphologies between the two alloys are different as shown in Fig. 3. Thus, even if the conditions of the SCWO test are at high temperature and pressure with the solution flowing in the reactor, it seems that the hardness of the samples is not the main factor for controlling the corrosion or erosion-corrosion behavior.

Fig. 5 shows the anodic polarization curves of base metal (non-SCWO tested) in 0.5 N HCl+1 N NaCl at room temperature. In the case of 316L, it did not show the passivity and was severely corroded. Duplex stainless steel, F255, revealed good passivity, and after a polarization test, no pits were observed, and thus the sharp increase of current density near 1 V (SCE) would be due to the oxygen evolution reaction. Generally, corrosion resistance of base metals is primarily important for predicting the resistance in certain environments. Totally, the lower the current density in

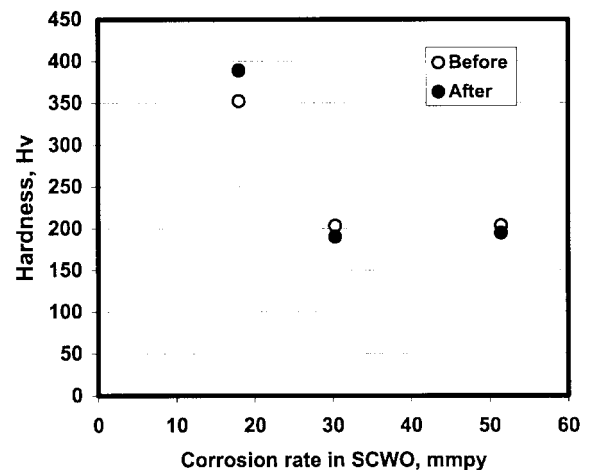


Fig. 4. Relationship between corrosion rate and hardness of stainless steels before/after SCWO test.

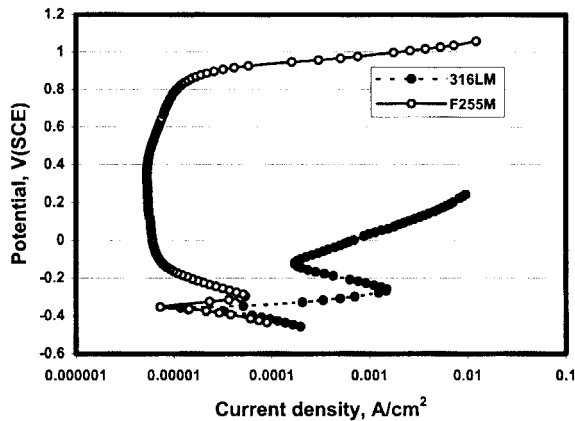


Fig. 5. Anodic polarization curves of austenitic and duplex stainless steels in 0.5 N HCl+1 N NaCl at room temperature.

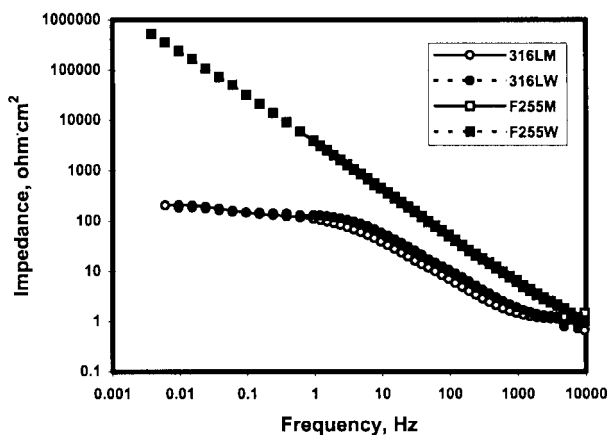


Fig. 6. EIS spectra of base/welded areas of stainless steels in 0.5 N HCl+1 N NaCl at room temperature.

anodic polarization curves, the better corrosion resistance in the SCWO test.

We did measure the AC impedance of the base metal and welded area of non-SCWO tested samples in 0.5 N HCl+1 N NaCl at room temperature. Fig. 6 shows the electrochemical impedance spectra of base metal and welded area, respectively. In the case of 316L, impedance value is lowest regardless of base and weld metal, but duplex stainless steel, F255, shows the higher impedance value.

Generally, we can predict the corrosion resistance in chloride environment by using PRE (Pitting Resistance Equivalent). Fig. 7 (upper) shows the relationship between corrosion rate in SCWO test and PRE $\{=Cr+3.3(Mo+0.5W)+30N\}$ value [Kim, 1998] of Ni-base [Kim, 1999] and Fe-base alloys. These four elements are very important in thin passive film formed at low temperature. As seen in the figure, there is no linear relationship between them. Even though this PRE equation is well applied to predict the corrosion resistance of stainless steel, the non-linearity of Fig. 7 (upper) implies that another factor has influenced the corrosion process in SCWO. Fig. 7 (lower) shows the relationship between Cr content of the alloy and corrosion rate in SCWO test of Ni-base [Kim, 1999] and Fe-base alloys. As shown in the figures, there is a closer relationship between corrosion rate in the SCWO test

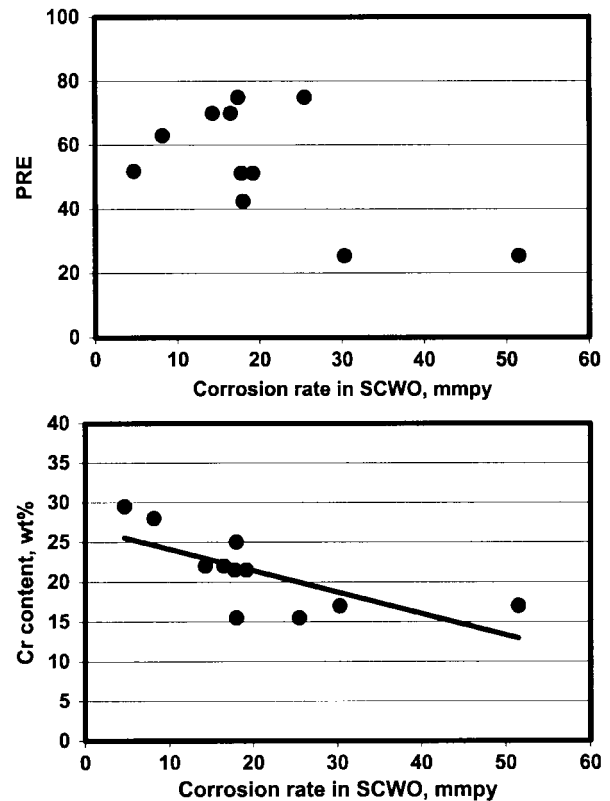


Fig. 7. Relationship between corrosion rate and PRE value (upper)/Cr content (lower) of Ni-based alloys [Kim, 1999] and stainless steels.

and Cr content of alloys.

Even though there is a close relationship between the Cr content and the corrosion rate, however, it should be explained how the Cr content could play an important role in corrosion behavior in the SCWO test.

2. Role of Oxide Formed on the Surface in SCWO Test

Oxide film formed on the surface in corrosive environments can generally protect against the attack from a corrosive solution. Passive film formed in low temperature and ambient pressure is usually very thin. The film consists of the enriched elements, such as Cr, Mo, W, N etc., and those four elements play very important roles in the passivation of stainless steels [Kim, 1992, 1998; Kim and Kim, 1997]. So, we can predict the corrosion resistance of certain alloys by using a PRE equation. However, as described earlier, this PRE equation could not give any information about the corrosion rate in the SCWO test. Probably, this is because SCWO test conditions are very high pressure and high temperature, even if it may be aqueous state.

In this work, we can postulate several situations about testing conditions as follows:

(1) Since testing temperature is 600 °C of supercritical condition, diffusion rate of alloying elements might be increased. So, a thick oxide layer can be formed rather than a thin passive film.

(2) Since testing solution is circulated at the rate of 2.2 kg/min, the solution would have a mechanical effect on the surface layer or corrosion products.

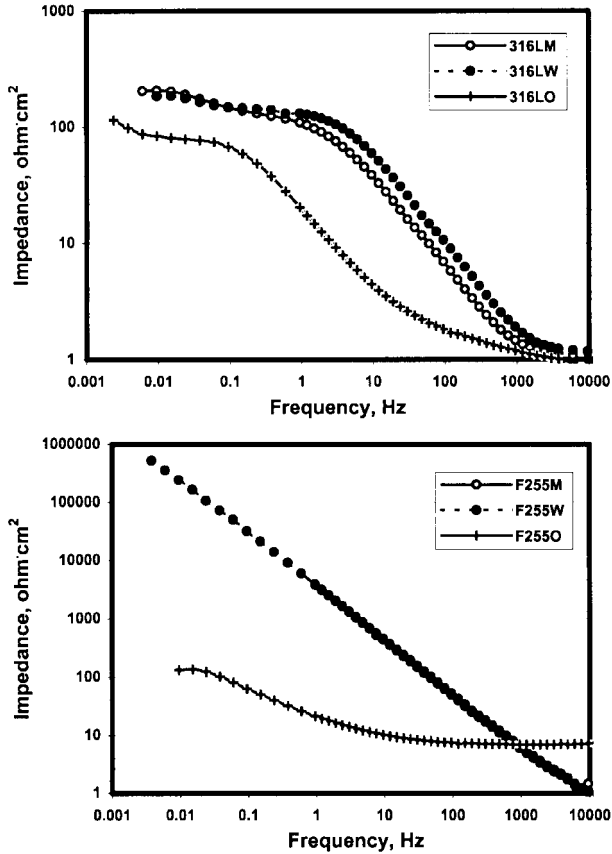


Fig. 8. Comparison of impedance between oxide-covered samples after SCWO test and base/welded area of austenitic (upper) and duplex (lower) stainless steels in 0.5 N HCl + 1 N NaCl at room temperature.

(3) In supercritical water conditions, a supercritical fluid reveals both gas- and liquid-like properties, and thus, this fluid may influence the corrosion of samples by an unknown process.

The black layer surface (in this work, we refer to this layer as oxide [O]) was formed on the surface. AC impedance measurement was performed for oxide-covered samples in 0.5 N HCl + 1 N NaCl under open circuit potential at room temperature. Oxide-covered sample was made by removal of salt layer by using ultrasonic cleaning in deionized water.

Fig. 8 (upper) shows the EIS spectra of austenitic stainless steel 316L, i.e., base metal, welded area, and oxide-covered sample. Fig. 8 (lower) shows the EIS spectra of duplex stainless steel F255, i.e., base metal, welded area, and oxide-covered sample. Oxide-covered samples show lower impedance than base and welded metals. This means this oxide layer is not protective. Also, in the case of Ni-based alloys, oxide-covered samples showed low impedance [Kim, 1999]. Fig. 9 (upper) reveals the relationship of $1/R_p$ value determined in 0.5 N HCl + 1 N NaCl at room temperature by EIS spectra between base metal and oxide-covered samples. $1/R_p$ was calculated from impedance spectra and this value is proportional to corrosion rate. As shown in the figure, $1/R_p$ (i.e. corrosion rate) of oxide-covered samples is larger than that of base metal. Moreover, Ni-based alloys, i.e., G30 and HR160, show the best corrosion resistance in the SCWO test, but the

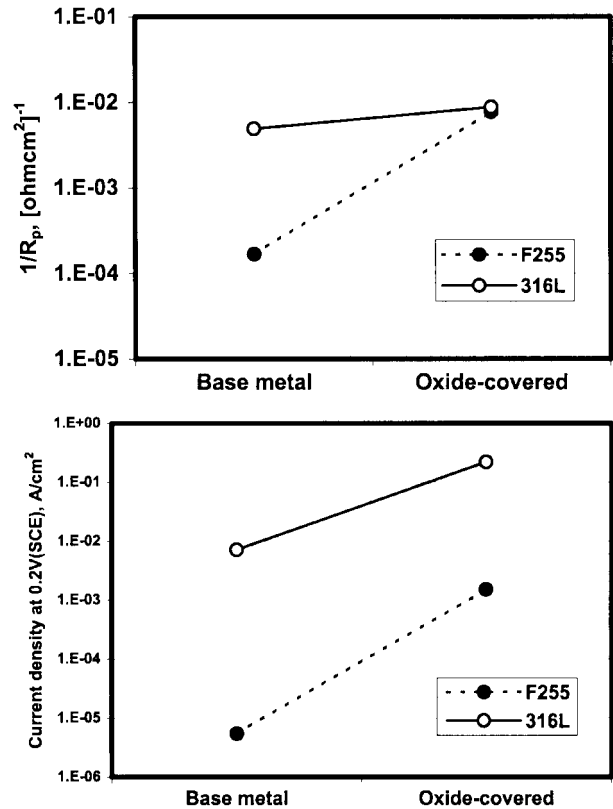


Fig. 9. $1/R_p$ (upper) obtained by EIS and current density (lower) at 0.2 V (SCE) obtained by anodic polarization test in 0.5 N HCl + 1 N NaCl at room temperature of stainless steels.

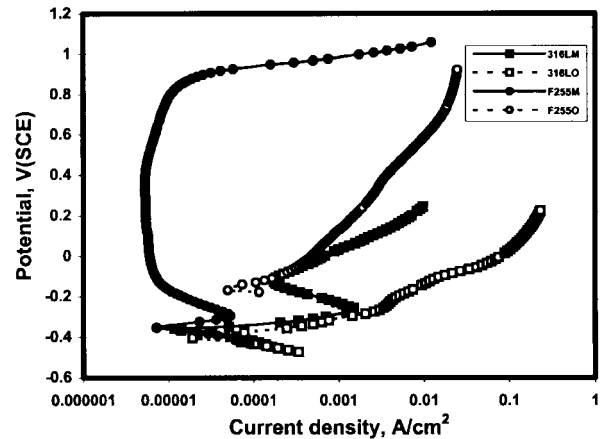


Fig. 10. Anodic polarization curves of base metals and oxide-covered samples in 0.5 N HCl + 1 N NaCl at room temperature.

oxide-covered samples of two alloys revealed higher $1/R_p$ value [Kim, 1999]. This result is not coincident with the high corrosion resistance in the SCWO test.

Fig. 10 shows the anodic polarization curves for oxide-covered samples in 0.5 N HCl + 1 N NaCl at room temperature. This is to compare the polarization behavior between base metal and oxide-covered samples. As seen in the figure, oxide-covered samples showed less corrosion resistance than the base metal. Also, Fig. 9 (lower) shows the current density at 0.2 V (SCE) of base

metal and oxide-covered samples. Like the impedance data of Fig. 9 (upper), the current density of oxide-covered samples is bigger than that of base metal. In summary, oxide-covered samples do not have good resistance compared to non-tested matrix (base metal)

samples, and this means the covered oxide may not protect the electrochemical or chemical attacks from supercritical water.

Figs. 11 and 12 show SEM image and WDS results for the cross section of 316L and F255 after SCWO test. In the case of

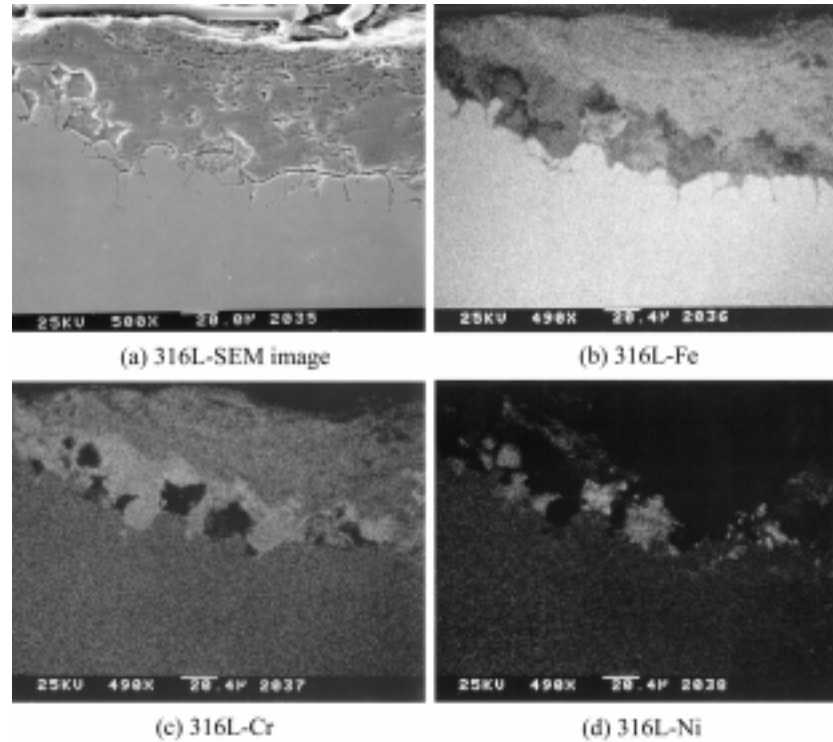


Fig. 11. SEM image and element distribution by WDS for austenitic stainless steel 316L after SCWO test.

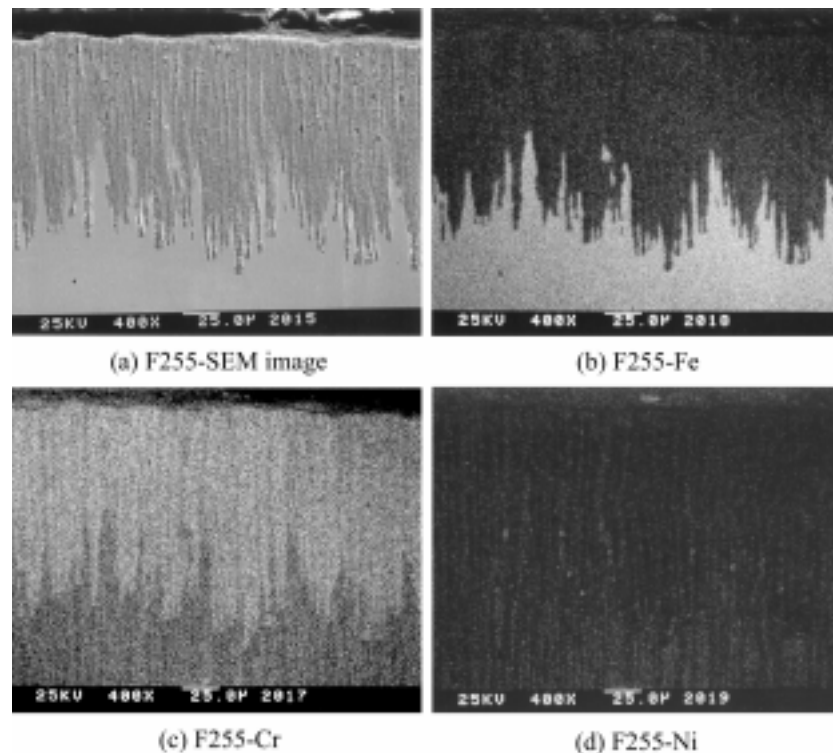


Fig. 12. SEM image and element distribution by WDS for duplex stainless steel F255 after SCWO test.

316L, intergranular corrosion was observed as with optical microscopic observation. The outer layer of oxide contains more Fe than Cr and the inner layer contains more Cr than Fe. However, nickel was locally enriched and this Ni-enriched area did not have Cr element. The oxide layer of 316L did not have uniform composition. Duplex stainless steel, F255 has two phases, austenite and ferrite, as shown in Fig. 3. By the result of OM, the rolling face was less corroded and it was hard to observe the oxide layer. However, we can easily observe the oxide layer in the end of rolling plate as shown in Fig. 12. Fe was selectively dissolved and Cr was enriched and Ni was almost constant in oxide layer of each phase. Oxide layer of F255 looks like more stable than that of 316L.

Duplex stainless steel F255 having shown the better corrosion resistance in SCWO test has a stable oxide layer on the surface, but austenitic stainless steel 316L having shown the worse resistance does not have a stable oxide layer on the surface. In the latter case, metal can easily diffuse into surface and dissolve directly into solution. Then, a dealloying layer could be formed on the surface, leading to the loss of a protective property (this was proved in Figs. 8, 9, 10). In other words, this layer did not act as a barrier layer against the attack in the SCWO test. Duplex stainless steel F255 shows a different behavior from Ni-base alloys. PRE value of F255 is 44.4 and this value is not high compared to Ni-base alloys (at least, above 50). Even though with a low PRE value of F255, its resistance is more excellent than 316L and similar to the rate of Ni-base alloys 625 and 276 [Kim, 1999]. As seen in OM, F255 could form a sort of stable diffusion layer and has two kinds of phases, hard phase-ferrite and soft phase-austenite, and its bulk hardness is the highest among the testing alloys. In SCWO test, these differences can make the corrosion resistance of alloy F255 higher.

CONCLUSIONS

1. Based on mass change, the corrosion rate of 316L in SCWO test was higher than that of F255.

2. In the case of 316L showing high corrosion rate in SCWO test, matrix was corroded and removed by intergranular corrosion and pitting. In the case of F255 showing good corrosion resistance, a stable oxide layer was formed on the surface.

3. In *ex-situ* DC polarization test and AC impedance measurement, the oxide-covered samples did not have good resistance compared to non-SCWO tested matrix samples; this means the covered oxide may not protect against the electrochemical or chemical attacks from supercritical water.

ACKNOWLEDGEMENT

This work was partly supported by the research fund of Andong National University and MIT, and we appreciate it.

REFERENCES

Aqua forties, US Army Research Office, **2**(2), (1993).
 Aqua forties, US Army Research Office, **2**(2), (1993b).
 Aqua forties, US Army Research Office, **3**(1), (1994).

ASM Handbook, Corrosion, 9th ed., Materials Park, OH, ASM International, **13**, 641 (1987).

Bramlette, T. T., Mills, B. E., Hencken, K. R., Brynildson, M. E., Johnston, S. C., Hruby, J. N., Feemster, H. C., Odegard, B. C. and Modell, M., "Destruction of DOE/DP Surrogate Wastes with Supercritical Water Oxidation Technology," Sandia National Laboratories Report, SAND90-8229 (1990).

Boukris, N., Landvatter, R., Habicht, W. and Franz, G., "First Experimental SCWO Corrosion Results of Ni-base Alloys Fabricated as Pressure Tubes and Exposed to Oxygen Containing Diluted Hydrochloric Acid at <450 °C, p=24 MPa," International Workshop on Supercritical Water Oxidation, Jacksonville, Florida, Feb. 6-9 (1995).

Drake, L., "Selecting Technologies for Destruction of the Chemical Weapons Stockpile," MIT Energy Laboratory Seminar, February (1993).

Kane, R. D. and Cuellar, D., "Literature and Experience Survey on Supercritical Water Corrosion," CLI International Report, No. L941079K, July 19 (1994).

Kim, Y. S., "An Investigation of Corrosion Mechanism and Techniques for Mitigation on SCWO System for Hazardous Waste Destruction," Final Report, Andong National University (1999).

Kim, Y. S., "Influences of Alloyed Molybdenum and Molybdate Addition on the Corrosion Properties and Passive Film Composition of Stainless Steels," *Metals and Materials*, **4**(2), 183 (1998).

Kim, Y. S., "Registration of SR-50A Super Austenitic Stainless Steel on Euronorm System," *J. of Corrosion Sci. Soc. of Korea*, **24**(3), 212 (1995).

Kim, Y. S., "The Influences of Nitrogen, and NO₃⁻, NO₂⁻, and NH₄⁺ Ions on the Corrosion Properties and Passive Film of Stainless Steels," *J. of Corrosion Sci. Soc. of Korea*, **21**(3), 189 (1992).

Kim, Y. S. and Kim, J., "The Influences of W and Mo Additions on the Pitting Resistance and the Passivation of Ferritic Stainless Steels," *J. of Corrosion Sci. Soc. of Korea*, **26**(6), 435 (1997).

Latanision, R. M. and Shaw, R. W., Co-Chairs, "Corrosion in Supercritical Water Oxidation Systems"-Summary of a Workshop Held at MIT May 6-7, 1993 (Report No. MIT-EL 93-006, 1993).

Latanision, R. M., "Corrosion Science, Corrosion Engineering and Advanced Technologies," *Corrosion*, **51**(4), 270 (1995).

Mitton, D. B., Orzalli, J. C. and Latanision, R. M., Proceedings of the Third International Symposium on Supercritical Fluids, France, October 17-19, 3, 43 (1994).

Mitton, D. B., Orzalli, J. C. and Latanision, R. M., "Physical Chemistry of Aqueous Systems-Meeting the Needs of Industry," 12th ICPWS, Begell House, New York, NY, 638 (1995a).

Mitton, D. B., Orzalli, J. C. and Latanision, R. M., "Science and Technology," ACS Symposium Series 608, ACS, Washington, DC, 327 (1995b).

Mitton, D. B., Zhang, S. H., Han, E. H., Hautanen, K. E. and Latanision, R. M., "Assessment of Corrosion and Failure Mechanisms in Supercritical Water Oxidation Systems," Proceedings of the 13th ICC, Melbourne, Australia, November 25-29 (1996a).

Mitton, D. B., Marrone, P. A. and Latanision, R. M., "Interpretation of the Rationale for Feed Modification in SCWO Systems," *J. Electrochem. Soc.*, **143**, L59 (1996b).

Mitton, D. B., Zhang, S. H., Quintana, M. S., Cline, J. A., Caputy, N., Marrone, P. A. and Latanision, R. M., "Corrosion Mitigation

- in SCWO Systems for Hazardous Waste Disposal," Paper No. 414, The Symposium on Corrosion in Supercritical Fluids, Corrosion 98, March 22-27, San Diego, CA (1998).
- Norby, B. C., "Supercritical Water Oxidation Bench-scale Testing Metallurgical Analysis Report," Idaho National Engineering Laboratory Report EGG-WTD-10675 (1993).
- Orzalli, J. C., "Preliminary Corrosion Studies of Candidate Materials for Supercritical Water Oxidation Reactor Systems," Master's Thesis, Department of Materials Science and Engineering, MIT (1994).
- Rice, S. F., Steeper, R. R. and LaJeunesse, C. A., "Destruction of Representative Navy Wastes Using Supercritical Water Oxidation," Sandia Report SAND94-8203 UC-402 (1993).
- Swallow, K. C. and Ham, D., "Hazardous Wastes," *The Nucleus*, 11 (1993).
- Swallow, K. W., Snow, R. H., Hazelebeck, D. A. and Roberts, A. J., "Science and Technology," ACS Symposium Series, 608, ACS, Washington, DC, 313 (1995).
- Tester, J. W., Holgate, H. R., Armellini, F. J., Webley, P. A., Killilea, W. R., Hong, G. T. and Barner, H. E., in Emerging Technologies for Waste Management III, ACS Symposium Series, 518, Washington, DC, ACS, 35 (1993).
- Tebbal, S. and Kane, R. D., "Materials Selection in Hydrothermal Oxidation Processes," Paper No. 413, The Symposium on Corrosion in Supercritical Fluids, Corrosion 98, March 22-27, San Diego, CA (1998).
- The Convention on the Prohibition of the Development, Production, Stockpiling and Use of Chemical Weapons and on their Destruction, Depository Notification C.N.246.1994. TREATIES-5 (1994).
- The NATO Advanced Workshop, "Destruction of Military Toxic Waste," Naaldwijk, the Netherlands, May 22-27, 1994; US Army Research Office Report (1994).
- Thomas, A. J. and Gloyna, E. F., "Corrosion Behavior of High Grade Alloys in the Supercritical Water Oxidation of Sludge," Technical Report CRWR 229, University of Texas at Austin (1991).
- Zilberstein, V. A., Bettinger, J. A., Ordway, D. W. and Hong, G. T., "Evaluation of Materials Performance in a Supercritical Wet Oxidation System," Corrosion 95, NACE, paper 558 (1995).